

THREE METHODS FOR PERFORMING HANKEL TRANSFORMS

R. A. Athale, H. H. Szu and J. N. Lee
Naval Research Laboratory, Washington, D. C. 20375

ABSTRACT

Generalized Hankel transforms are useful in analyzing the effect of circularly symmetric optical systems on arbitrary inputs. Some examples of such systems are complex laser resonators and space telescopes. Three methods for performing Hankel transforms with optical or digital processors are described. The first method is applicable when the input data is available in Cartesian (x-y) format and uses the close connection between generalized Hankel transform and the two-dimensional Fourier transform in Cartesian coordinates. The second method is useful when the input data is in polar (r - θ) format and uses change of variables to perform the n^{th} order Hankel transform as a correlation integral. The third method utilizes the von Neumann addition theorem for Bessel functions to extract the Hankel coefficients from a correlation between the radial part of the input and a Bessel function. Initial experimental results obtained for optical implementation of the first two methods are presented.

INTRODUCTION

The analysis of complex optical systems is greatly facilitated by two-dimensional Fourier transform techniques. The effect of an optical system on arbitrary inputs is easily described by a transfer function in the Fourier domain. Generalized Hankel transforms are similarly useful when dealing with a circularly symmetric (or axisymmetric) system for arbitrary inputs.¹ This situation is encountered in performing mode analysis on the output of a slightly misaligned laser resonator as well as in aligning space telescopes. An optical method for performing mode analysis via generalized Hankel transform will have the unique advantage of preserving the phase of the wavefront to be analyzed.

It is well known that when a two-dimensional function has circular symmetry (i.e. it depends only on the radial variable, r), its Fourier transform is also circularly symmetric (i.e. it depends only on the radial variable, ρ). It can be shown that in such a case the Fourier transform is equivalent to the 0th order Hankel transform.²

If

$$f(x,y) \equiv f\left(\sqrt{x^2+y^2}\right)$$

Then

$$\mathcal{F}_2 \left\{ f\left(\sqrt{x^2+y^2}\right) \right\} = \mathcal{F}\left(\sqrt{u^2+v^2}\right)$$

where $\mathcal{F}_2 \{ \}$ indicates two-dimensional Fourier transformation.

For

$$r = \sqrt{x^2 + y^2}, \quad \rho = \sqrt{u^2 + v^2}$$

$$\mathcal{F} \left(\sqrt{u^2 + v^2} \right) \equiv F_0(\rho) = 2\pi \int_0^\infty r dr f(r) J_0(\rho r) \quad (1)$$

where $F_0(\rho)$ is the 0th order Hankel transform and $J_0(\rho r)$ is the 0th order Bessel function of the first kind. Thus in dealing with circularly symmetric systems, the 0th order Hankel transform (which is a one-dimensional operation) can be used instead of the two-dimensional Fourier transform if the inputs also are circularly symmetric. For arbitrary inputs, this technique can be extended by using the generalized Hankel transform, which expands on the nth order transform ($F_n(\rho)$ with kernel $J_n(\rho r)$ in Eq. (1)).

The generalized Hankel transform, $F_{nn}(\rho)$, can be defined for an arbitrary function, $f(r, \theta)$, as follows:

$$f(r, \theta) = \sum_{n=-\infty}^{\infty} f_n(r) e^{jn\theta} \quad (2)$$

$$F_{nn}(\rho) = \int_0^\infty r dr f_n(r) J_n(\rho r)$$

The generalized Hankel transform thus involves a Fourier series expansion in θ , followed by an nth order Hankel transform (with nth order Bessel function, $J_n(\rho r)$, as the transformation kernel) on the nth coefficient of expansion, $f_n(r)$. This generalized Hankel transform is useful in analyzing systems with circular symmetry but when the input is not circularly symmetric.

In the following sections we will describe three techniques for easy implementation of the generalized Hankel transform with optical or digital processors. These three techniques are each applicable in different circumstances. Initial experimental results on the optical implementation of the first two methods will be presented. In conclusion, we will detail the course of future work in this area.

OPTICAL IMPLEMENTATION OF GENERALIZED HANKEL TRANSFORM

In optical processors a two-dimensional Fourier transform with respect to the Cartesian coordinates (x, y) is performed very easily with the help of a simple spherical lens.² The equivalence of two-dimensional Fourier transform and 0th order Hankel transform for circularly symmetric functions was established in the Introduction. A similar connection exists between two-dimensional Fourier transform with respect to Cartesian coordinates (x, y) and nth order Hankel transform of the radial part if the function is of a form $f(r) e^{jn\theta}$.

$$\mathcal{F}_2 \left\{ f(r) e^{jn\theta} \right\} = 2\pi F_n(\rho) e^{-jn\phi} \quad (3)$$

where

$$\rho = (u^2 + v^2)^{1/2}, \quad \phi = \tan^{-1}(v/u).$$

and by definition

$$F_n(\rho) = \int_0^{\infty} r dr f(r) J_n(\rho r).$$

This connection arises out of the integral representation of $J_n(\rho r)$.¹ Using this result in the definition of generalized Hankel transform given in Eq. (2) the following relation is obtained between the two-dimensional Fourier transform and the generalized Hankel transform:

$$\begin{aligned} \mathcal{F}_2 \left\{ f(r, \theta) \right\} &= \mathcal{F}_2 \left\{ \sum_{n=-\infty}^{\infty} f_n(r) e^{jn\theta} \right\} \\ &= 2\pi \sum_{n=-\infty}^{\infty} F_{nn}(\rho) e^{-jn\phi} \end{aligned} \quad (4)$$

Thus the generalized Hankel transform $F_{nn}(\rho)$ is equivalent to the n^{th} coefficient of Fourier series expansion of $\mathcal{F}(\rho, \phi)$ in variable ϕ . Using this result, an optical system shown in Fig. 1 is designed to perform generalized Hankel transform on an arbitrary input that is available in Cartesian format ($f(x, y)$). The spherical lens performs a two-dimensional Fourier transform on $f(x, y)$ generating $\mathcal{F}(u, v)$. A suitably designed computer generated hologram then performs the Cartesian-to-polar ($u, v \rightarrow \rho, \phi$) coordinate transformation on $\mathcal{F}(u, v)$ generating $\mathcal{F}(\rho, \phi)$.³ This is followed by a cylindrical lens which takes a one-dimensional Fourier transform with respect to variable ϕ generating the desired output, $F_{nn}(\rho)$.

Initial optical experiments established the connection between two-dimensional Fourier transform and n^{th} order Hankel transform for a function of the form $f(r)e^{jn\theta}$. The schematic diagram of the optical system is shown in Fig. 2. A computer generated hologram was used to encode $e^{jn\theta}$ dependence of the input. The output was detected by a TV camera, which measures the light intensity in the Fourier plane of the input. The input used in these experiments had an r dependence given by $\delta(r-a)$, thus corresponding to a thin ring of radius "a" in the Cartesian (x, y) plane. The n^{th} order Hankel transform of $\delta(r-a)$ is $aJ_n(a\rho)$, making the output easily understandable. Figure 3 shows the results corresponding to 0^{th} order Hankel transform (i.e. $e^{jn\theta} = 1$). In Fig. 3(b) the function $|J_0(a\rho)|^2$ is plotted, which is then compared to a line scan through

the origin (Fig. 3(c)) of the output shown in Fig. 3(a). Very good qualitative agreement between the theoretical and experimental results is obtained. Figures 4(a-c) present the results for 1st order Hankel transform for the same $f(r)$, but here the θ dependence is $e^{j\theta}$. Again good qualitative agreement is seen between theory and experiment. A line scan through the origin of the output corresponding to 2nd order Hankel transform of $\delta(r-a)$ (with θ dependence $e^{j2\theta}$) is shown in Fig. 5. The zero at the origin was broader and the side lobes were seen to fall slower indicating that we indeed have $|J_2(a\rho)|^2$ as expected.

OPTICAL IMPLEMENTATION OF NTH ORDER HANKEL TRANSFORM

The previous method is applicable when the input is available in Cartesian (x,y) format, since it involves performing two-dimensional Fourier transforms with respect to the Cartesian variables. If the input is polar (r, θ) formatted, a more direct approach outlined in Eq. (3) has to be followed in obtaining generalized Hankel transform. The first part of the operation, which involves a Fourier series expansion in variable θ , is easily performed optically using a cylindrical lens. The calculation of nth order Hankel transform of the nth coefficient of expansion is less straightforward since it corresponds to a space-variant operation. So the main aim of the next two methods is to perform the space-variant operation of nth order Hankel transform optically.

a. Method Using Change of Variables

One standard procedure used in converting a space-variant operation into a shift-invariant operation is to employ appropriate change of variables. In the case of nth order Hankel transforms the following procedure was described by Siegman for implementing the space-variant operation as a correlation integral on a digital processor.⁴ From the definition

$$F_n(\rho) = \int_0^{\infty} r dr f(r) J_n(\rho r),$$

using

$$r = r_0 e^{\alpha x}, \quad \rho = \rho_0 e^{\alpha y} \tag{5}$$

$$\hat{F}_n(y) = \int_{-\infty}^{\infty} \hat{f}(x) \hat{J}_n(x+y) dx$$

where $\hat{F}_n(y) = \rho F_n(\rho)$, $\hat{f}(x) = r f(r)$, and $\hat{J}_n(x+y) = \alpha r \rho J_n(r\rho)$. The algorithm, therefore, consists of first linearly weighting the input $f(r)$ and performing $r \rightarrow x$ (logarithmic related) coordinate transform. This distorted input is then correlated with a similarly weighted and coordinate-transformed nth order Bessel function to give the desired Hankel transform as well as linearly weighted and coordinate distorted forms. In any physical system the correlation integral will be performed over a finite interval, giving rise to truncation errors. Also if the input is sampled in the x-domain, the sampling rate should be adequate to represent the function accurately in x-domain.

These factors and others are discussed at length, especially for digital implementation, in Refs. 4 and 5.

Since the operations of coordinate transformation and correlation can be performed by an optical processor, the optical system outlined in Fig. 6 can calculate n^{th} order Hankel transforms. Computer generated holograms are used to perform $r \rightarrow x$ coordinate transformation as well as to encode the Fourier plane filter with impulse response $\hat{J}_n(x)$. The second dimension of the optical processor can be used to perform different order Hankel transforms on different inputs, thus achieving multichannel operation.

In the initial experiment, both the input and the Fourier plane filter were encoded by computer generated holograms. The linear weighting and the coordinate transformation of the input was performed by the digital computer before doing the holographic encoding. The computer generated holograms used the Lee-Burckhardt technique⁶ and contained 128 pixels. The optical system is depicted in Fig. 7. This system was then used to perform 0th order Hankel transform on two different inputs, $f_1(r) = \rho_1 J_0(\rho_1 r)$ and $f_2(r) = \rho_2 J_0(\rho_2 r)$. The result of 0th order Hankel transform on $f_1(r)$ and $f_2(r)$ should be $\delta(\rho - \rho_1)$ and $\delta(\rho - \rho_2)$ respectively. The results of the computer simulation of this algorithm are depicted in Fig. 8. The finite width of the peak and the sidelobes are due to the finite limits of integration. To facilitate easy comparison with the experimental results, the 0th order Hankel transform with linear weighting and coordinate distortion (i.e. $|\hat{F}_0(y)|^2$) was plotted versus y instead of $F_0(\rho)$ versus ρ . Figure 9 shows the experimental results obtained. The optical output was detected by a 1024-element Reticon linear photodiode array. The shift in the peak position and the difference in the peak heights (due to the linear weight) are evident, indicating good qualitative agreement with the computer simulation results.

b. Method Using Neumann Addition Theorem

This method investigates an approach based on the special properties of Bessel functions.⁷ If the input $f(r)$ is correlated with $J_m(\rho r)$ then the m^{th} order Hankel coefficient $F_m(\rho)$ is obtained at the origin of the correlation plane for the particular value of ρ encoded in the Bessel function kernel.

$$F_m(\rho) = \int_0^{\infty} r dr f(r) J_m(\rho(r+r')) \Big|_{r'=0} \quad (6)$$

The Neumann addition theorem for Bessel functions states that

$$J_m(\rho(r+r')) = \sum_{n=-\infty}^{\infty} J_{m-n}(\rho r') J_n(\rho r) \quad (7)$$

Substituting for $J_m(\rho(r+r'))$ from Eq. (7) into Eq. (6) we get

$$\begin{aligned}
\int_0^{\infty} r dr f(r) J_m(\rho(r+r')) &= \int_0^{\infty} r dr f(r) \sum_{n=-\infty}^{\infty} J_{m-n}(\rho r') J_n(\rho r) \\
&= \sum_{n=-\infty}^{\infty} J_{m-n}(\rho r') F_n(\rho).
\end{aligned} \tag{8}$$

Thus it is seen that the correlation plane contains an infinite sum of Bessel functions of different order weighted by Hankel transform coefficients of different order. So in principle it is possible to extract Hankel transform coefficients of different order out of a single one-dimensional correlation operation.

The other dimension of optical system can be used to perform correlations with $J_m(\rho r)$ with different values of ρ to obtain complete Hankel transform. This approach is currently being evaluated further to determine the situations in which this method will be suitable.

FUTURE WORK

In this paper we have presented brief outlines of three different approaches for performing generalized Hankel transforms by optical or digital processors. We also presented initial experimental results on two of the three approaches. The future work will concentrate on carrying out the coordinate transformation required by the first two methods optically via computer generated holograms. A more quantitative analysis of the performance of the optical processor will be carried out. These three methods will be compared with each other with respect to space-bandwidth requirements as well as pre- and post-processing requirements. Finally, generalized Hankel transforms will be applied to specific problems, such as analysis of complex laser resonators, and optical systems will be developed for those problems.

ACKNOWLEDGEMENT

We wish to thank Dr. J. R. Leger for producing the computer generated holograms using the facilities at University of California, San Diego.

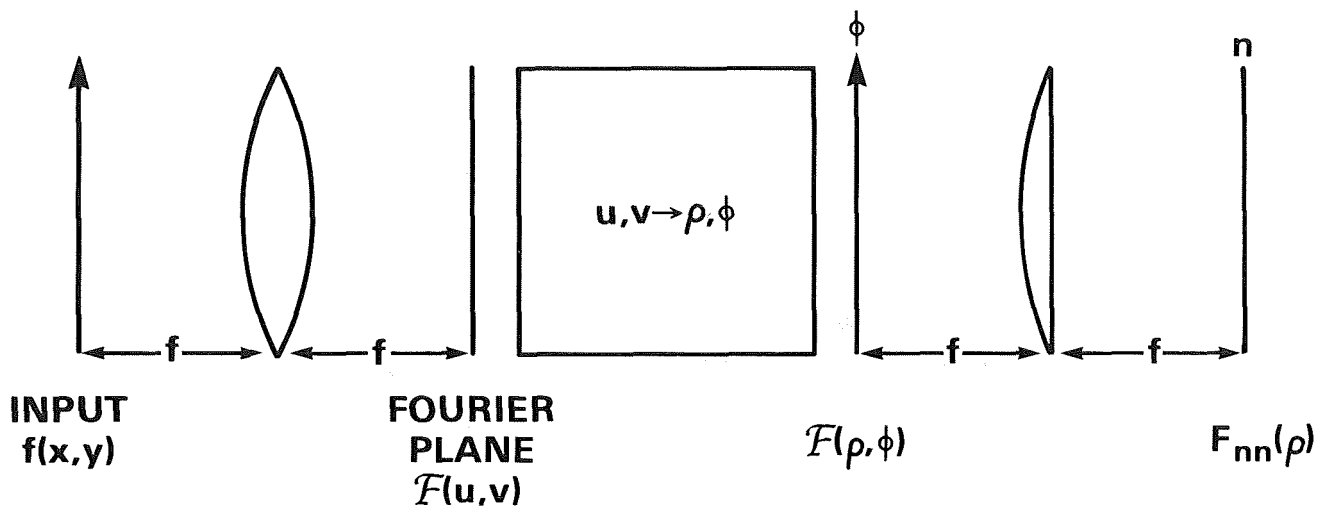


Figure 1. - Schematic diagram of optical processor for performing generalized Hankel transform via a two-dimensional Fourier transform with respect to Cartesian coordinates (x,y) .

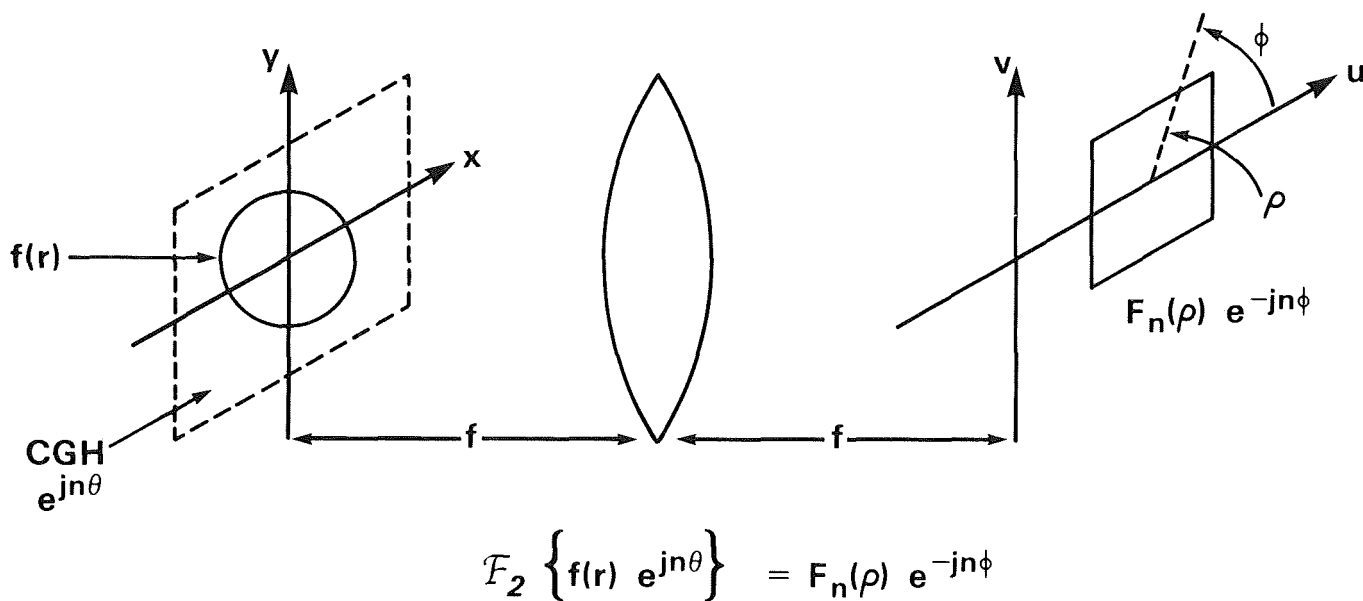
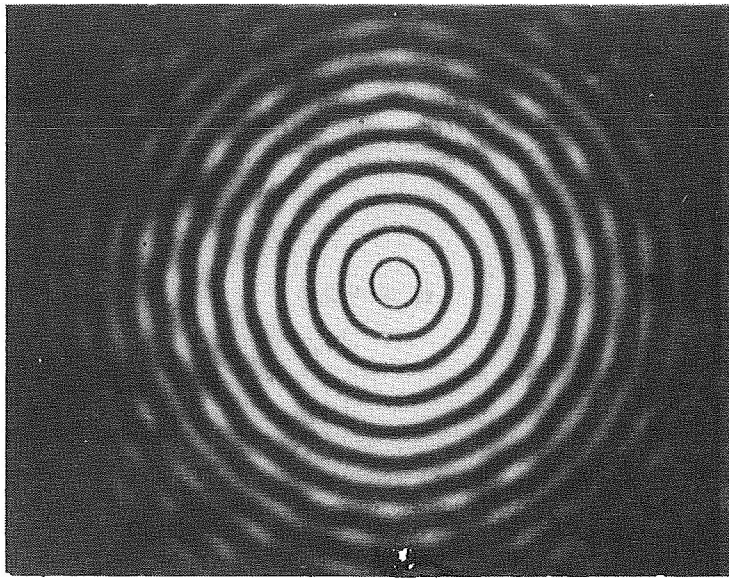
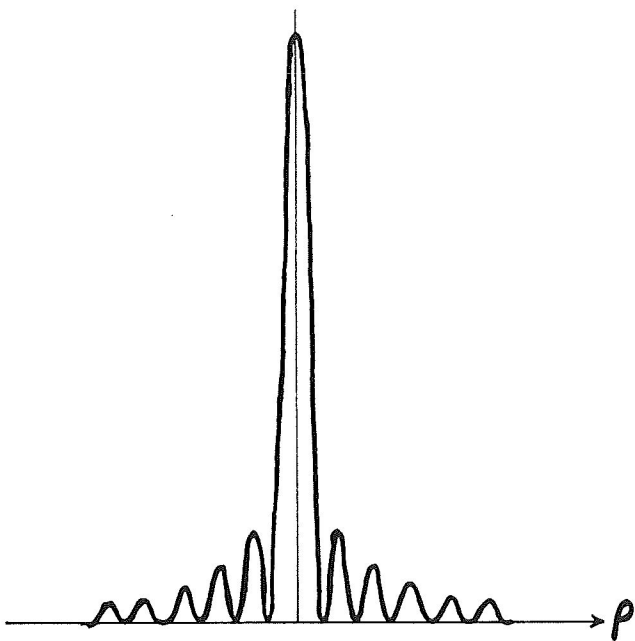


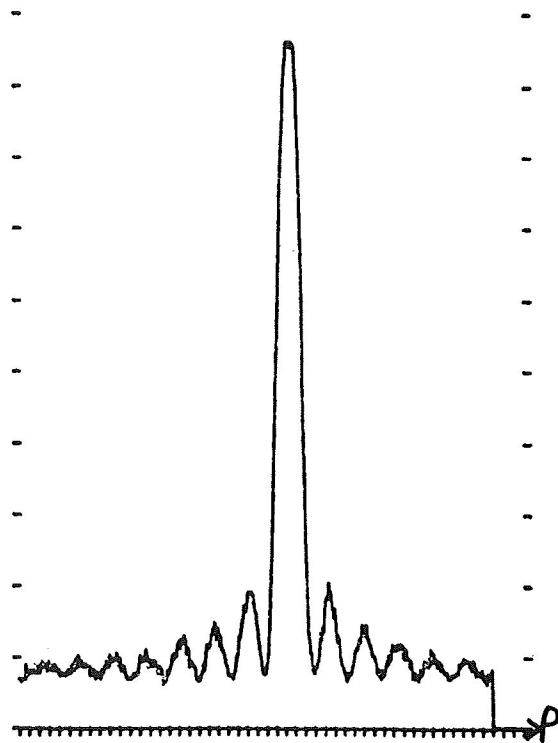
Figure 2. - Schematic diagram of experimental setup for establishing the relation between n^{th} order Hankel transform of $f(r)$ and two-dimensional Fourier transform of $f(r) e^{jn\theta}$ with respect to Cartesian coordinates (x,y) .



(a) Photograph of the output.

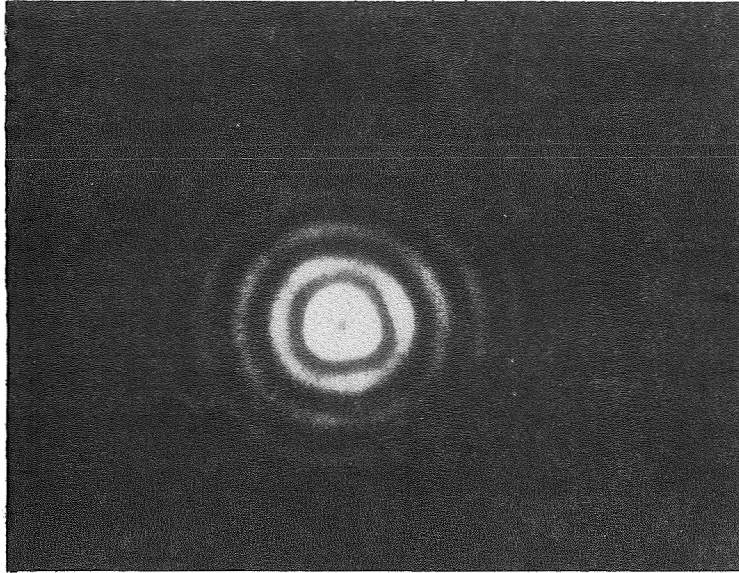


(b) Plot of $|J_0(a\rho)|^2$ versus ρ , which is the theoretically expected result.

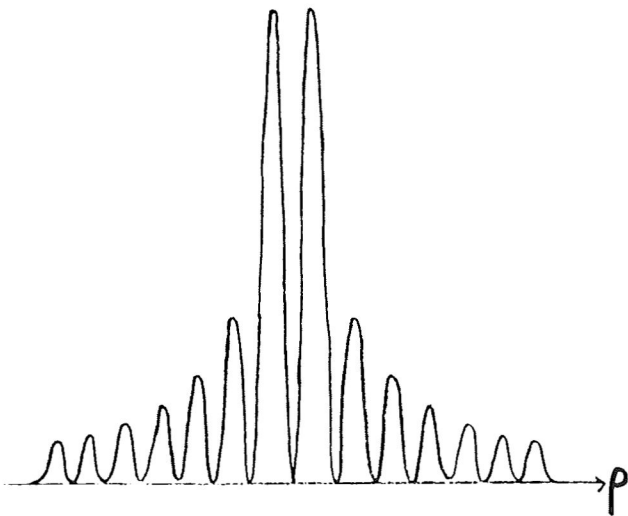


(c) Line scan through the origin of the pattern in figure 3 (a), giving $|F_0(\rho)|^2$ versus ρ .

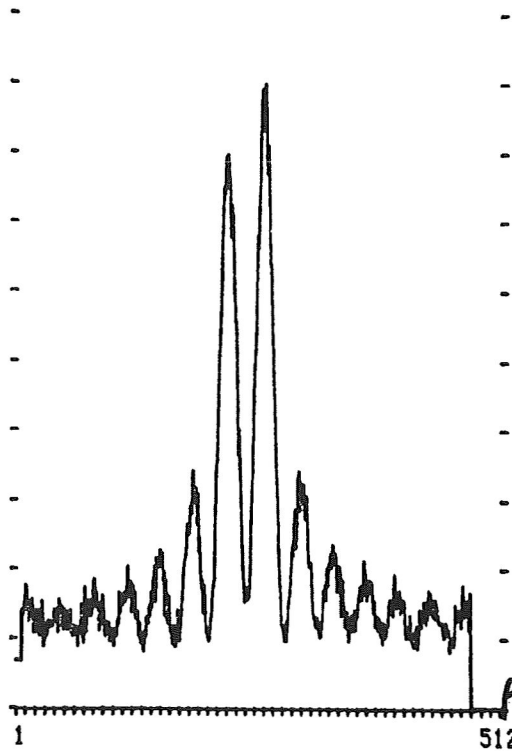
Figure 3. - Experimental results for 0th order Hankel transform $F_0(\rho)$ of $\delta(r-a)$.



(a) Photograph of the output.



(b) Plot of $|J_0(a\rho)|^2$ versus ρ , which is the theoretically expected result.



(c) Line scan through origin of the bottom in figure 4 (a), giving $|F_1(\rho)|^2$ versus ρ .

Figure 4. - Experimental results for 1st order Hankel transform $F_1(\rho)$ of $\delta(r-a)$.

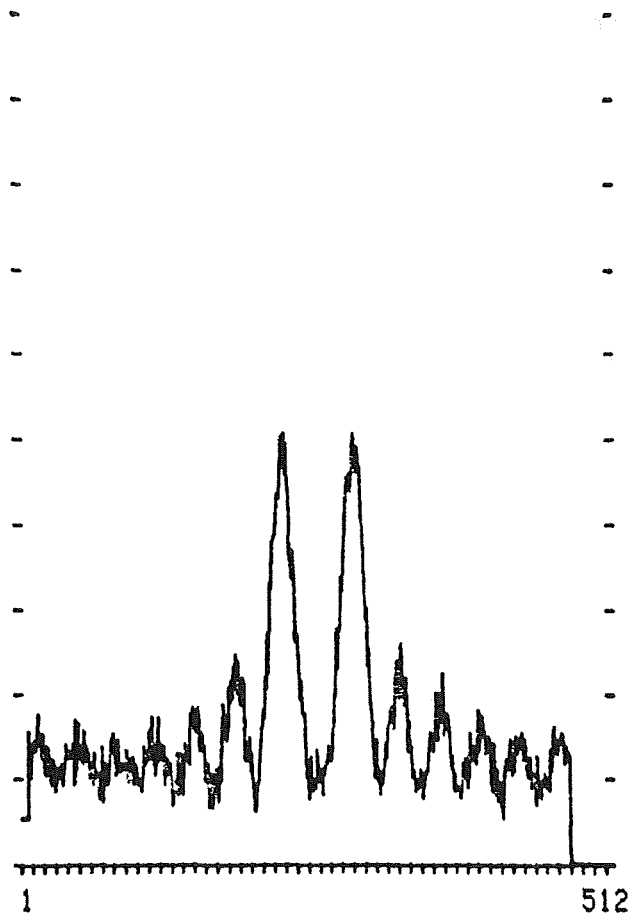


Figure 5. - Line scan through the origin of the two-dimensional Fourier transform of $\delta(r - a) e^{j2\theta}$, giving $|F_2(\rho)|^2$ for $\delta(r - a)$.

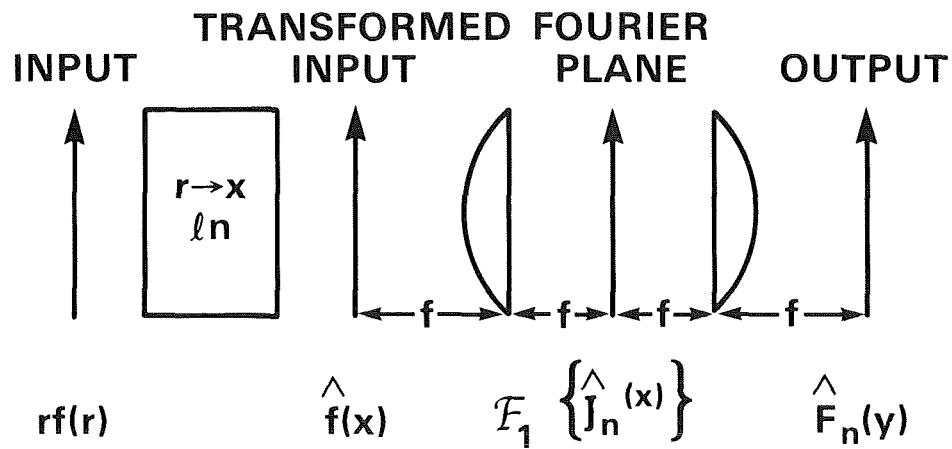


Figure 6. - Schematic diagram of an optical processor for performing n^{th} order Hankel transform on $f(r)$ employing change of variables.

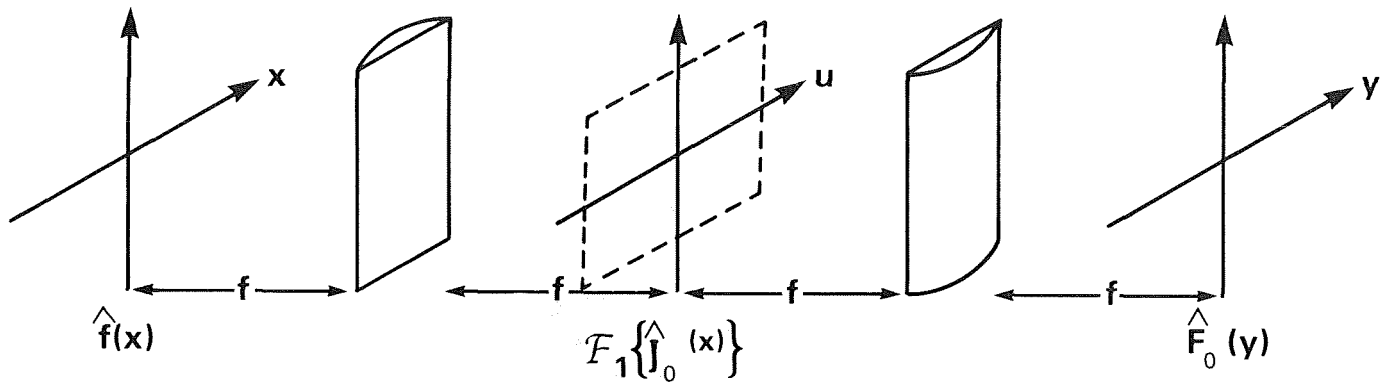


Figure 7. - Schematic diagram of the experimental setup for performing the one-dimensional correlation between linearly weighted and coordinate transformed input, $\hat{f}(x)$, and similarly weighted and transformed Bessel function $\hat{J}_0(x)$.

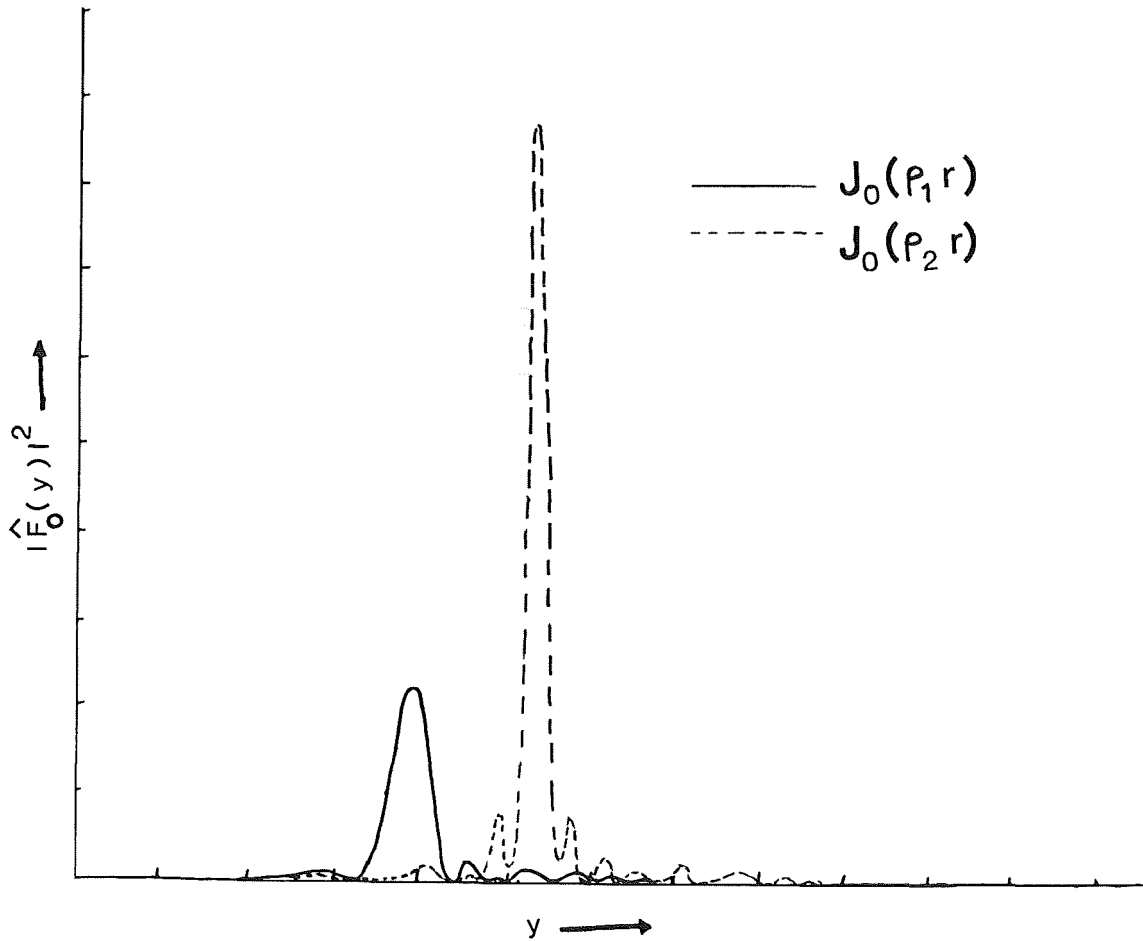
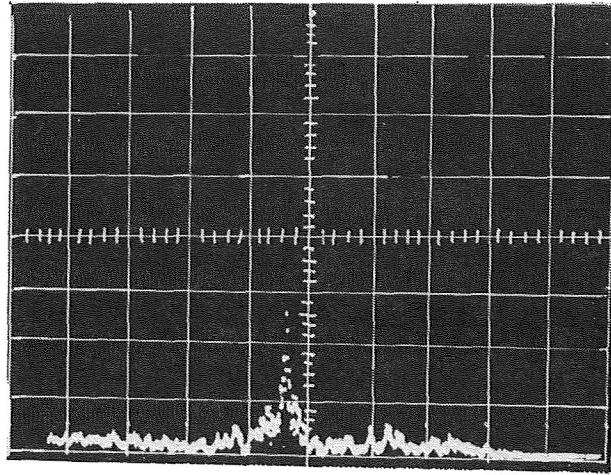
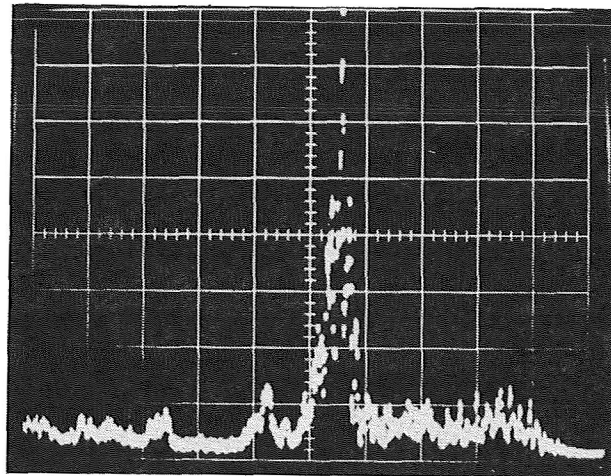


Figure 8. - Results of computer simulation of 0th order Hankel transform of $\rho_1 J_0(\rho_1 r)$ and $\rho_2 J_0(\rho_2 r)$. The linearly weighted and coordinate transformed Hankel coefficients, $|\hat{F}_0(y)|^2$, are plotted versus y . $\rho_2 = 2\rho_1$.



(a) Input $f_1(r) = \rho_1 J_0(\rho_1 r)$.



(b) Input $f_2(r) = \rho_2 J_0(\rho_2 r)$.

Figure 9. - Oscilloscope traces of output of the optical processor performing the 0th order Hankel transform. Traces correspond to $|\hat{F}_0(y)|^2$ versus y for the two inputs.